5R.7 RELATIVE ERRORS IN TRMM SATELLITE VERSION 5 AND VERSION 6 PRODUCTS: STEPS FORWARD AND BACKWARD

Sandra E. Yuter*[1], John Stout[2], Robert Wood[3], John Kwiatkowski[2], and Daniel Horn[1]
[1]North Carolina State University, Raleigh, NC
[2]George Mason University, Fairfax, VA
[3]University of Washington, Seattle, WA

1. INTRODUCTION

The Tropical Rainfall Measuring Mission (TRMM) satellite (Kummerow et al. 1998) has yielded estimates of surface rainfall over the global tropics since shortly after the TRMM launch in November 1997. The TRMM mission is an international research initiative lead jointly by NASA and the Japanese space agency JAXA (previously called NASDA). The TRMM satellite includes a multi-frequency passive microwave radiometer (TRMM Microwave Imager—TMI) and a 13.8 GHz frequency precipitation radar (PR) permitting simultaneous and independent measurements of storm characteristics between 35 S and 35 N latitude.

The TRMM satellite precipitation retrieval algorithms have undergone a series of refinements since launch that have been released intermittently and labeled with different version numbers. TRMM Version 5 (V5) was released in November 1999 and Version 6 (V6), the most recent version, was released in April 2004.

While the changes incorporated into each new version are intended to improve the TRMM products' accuracy and precision, they do not always do so across all metrics. The impact of precipitation retrieval errors varies with the product application. This paper will characterize several types of relative errors between TMI and PR precipitation retrievals in V5 and V6 products.

Error characteristics associated with satellite-derived precipitation products are important for the integration of TRMM products in numerical model data assimilation, forecasting, and climate diagnostics applications. Additionally, this information aids in the diagnosis and refinement of physical assumptions within algorithms by identifying geographic regions and seasons where existing algorithm physics may be incorrect or incomplete. Examination of relative errors between independent estimates derived from satellite passive microwave and precipitation radar is particularly important over regions with limited surface-based measurements of rain rates such as the global oceans and tropical continents. Ground-based observations at selected sites can help guide the physical interpretation of the error characteristics.

This analysis of TRMM satellite data sets yields error information on the current TRMM products. Additionally, use of TRMM products provides an opportunity to prototype global error characterization methodologies for the TRMM follow-on program, the Global Precipitation Measurement (GPM) mission, to be launched sometime in the future.

The TRMM satellite completes a full sampling of the diurnal cycle every 47 days. When possible we use 47-day or 3-month (~2 x 47 days) periods to minimize the aliasing of diurnal precipitation variations into our results. The TRMM satellite orbit was increased from 350 km to 402 km altitude in August 2001. Time periods before August 2001 are referred to as "pre-boost" and those after as "post-boost".

2. DATA SETS

The TRMM satellite data sets are processed to yield several types of relative error statistics in this study. We also examine the plausibility of the TRMM products compared to existing empirical knowledge. TMI and PR instantaneous rain rates are compared over ocean and land in V5 and V6 using orbit data from TRMM products 2A-12, representing the TMI rainfall retrieval, and 2A-25, representing the PR rainfall retrieval. Ocean pixels are separated from land pixels because the weighting of TMI passive microwave channels within the precipitation retrieval is sufficiently

* *Corresponding author address:* Sandra E. Yuter, North Carolina State University, Dept. of Marine, Earth and Atmospheric Sciences, Raleigh, NC 27695; e-mail: sandra_yuter@ncsu.edu.

different over ocean versus land to yield distinct algorithm physics (Smith et al. 1998). Passive microwave scattering from ice is used as a proxy for rain to estimate surface rainfall over land while over ocean both emission and scattering channels are used.

Since precipitation rates vary with spatial scale (Tustison et al. 2001), the PR pixels are used both at their native sensor resolution of 4.3 km (pre-boost) or 5 km (post-boost) and are upscaled to TMI spatial scales for comparison. Within the TMI instantaneous algorithm 2A-12, 85 GHz and 19 GHz are the heaviest weighted channels over land and ocean respectively (Kummerow, 2004, personal communication). We use the "near surface" values for rain rates which are available in both V5 and V6 products.

Three-month averages of 5° x 5° TRMM monthly products 3A-25 (for PR) and 3B-31 (for TMI) over 4 years are used to examine relative changes in the global and seasonal climatologies between V5 and V6. In addition, midtropospheric vertical velocity (500 hPa pressure velocity, $_{500}$ in hPa day^{-1}) from NCEP reanalysis and SST from the Reynolds SST optimally interpolated product from NCEP are used in a compositing analysis following Williams et al. (2003) and Bony et al. (2004).

3. GLOBAL PDF COMPARISONS

Examination of the probability density function (PDF) of surface rain rates yields both physical plausibility as well as relative error information. It is well known that observed rainfall rates are unimodal with a roughly Gaussian distribution in dBR=10*log10(R) space where R is rain rate in mm hr^{-1}. Implausible deviations of the PDF of dBR from a Gaussian distribution are indications of serious problems. Figure 1 shows global tropical comparison of PDFs of PR vs. TMI rainfall estimates over ocean and land for August 1998. Over ocean the TMI vs. PR PDFs shifted closer together between V5 and V6 (Fig. 1a). The TMI V5 land PDF fails the plausibility test (Fig. 1b) as it is discontinuous, i.e., rain rates between 0.5 to 1.3, 1.6 to 2.5, and 3.2 to 5 mm hr^{-1} never occur! The TMI land PDF is substantially improved in V6 as it is now at least roughly the correct shape. Large discrepancies in the frequency of rain rates < 0.4 mm hr^{-1} are present between PR and TMI over land in V6. These discrepancies are likely related to differences in minimum detectable rain rates between the TMI pixels and the rescaled PR pixels. The PDF of PR rain rates over land changed very little between V5 and V6.

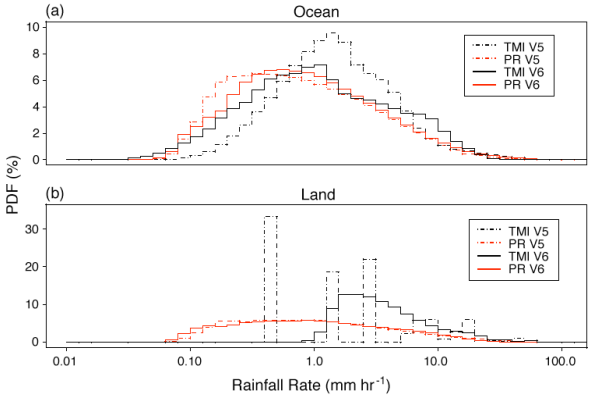

Fig. 1. *PDF instantaneous rain rates from TMI and PR orbit data for (a) global ocean and (b) global land based on TRMM products 2A-12 (TMI) and 2A-25 (PR) during August 1998. PR data are rescaled to the TMI 85 GHz spatial scale of 4 km x 7 km.*

4. REGIONAL SEASONAL CYCLE

Figure 2 shows several estimates of the seasonal cycle of precipitation over the eastern Pacific ITCZ (145 to 100°W longitude and 0 to 20°N latitude) determined from TMI and PR 5° x 5° data obtained before the satellite's orbit boost in August 2001. The relative differences in mean values are smaller between V6 as compared to V5 and the seasonal modulation is essentially unchanged from V5 to V6. In V6, there are differences between PR and TMI in the timing of the local minimum of precipitation in 1999 and 2000. Additionally, the fall season precipitation magnitudes differ in the seasonal average from 0.3 to 0.8 mm hr^{-1}. The differences in sampling related to different swath widths of PR and TMI are not a major source of discrepancies in the

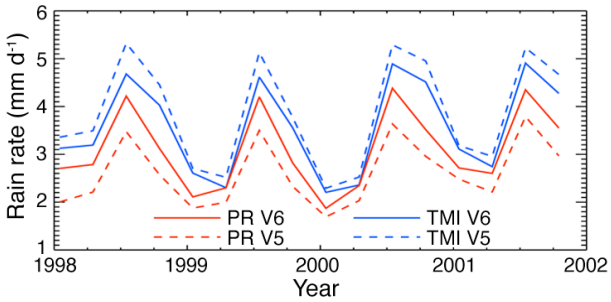

Fig 2. *TRMM satellite estimates of oceanic precipitation seasonal cycle for the eastern Pacific ITCZ (145 to 100°W longitude and 0 to 20°N latitude) based on 3-month averages of monthly products (TMI) 3B-31 and 3A-25 (PR) from 1998-2002.*

seasonal cycle. TMI full swath and the subset of TMI overlapping the PR swath have nearly identical seasonal cycles.

5. COMPOSITING ANALYSIS

To better understand the possible sources of the TRMM oceanic rain rate changes, we examine a decomposition of satellite-retrieved rain rate by $_{500}$ and SST following Williams et al. (2003) and Bony et al. (2004). This type of display organizes information on the differences between V5 and V6 in terms of the large-scale environmental characteristics of midtropospheric vertical velocity, $_{500}$ and SST. $_{500}$ is negative for upward motion and positive for downward motion. Hence the heaviest oceanic precipitation is expected in regions with highest SST and lowest $_{500}$ (upper left of composite figures). Figure 3 shows the average rain rate difference in TMI and PR between V6 and V5. For TMI V6-V5, regions of high SST (>26°C) and upward motion show a

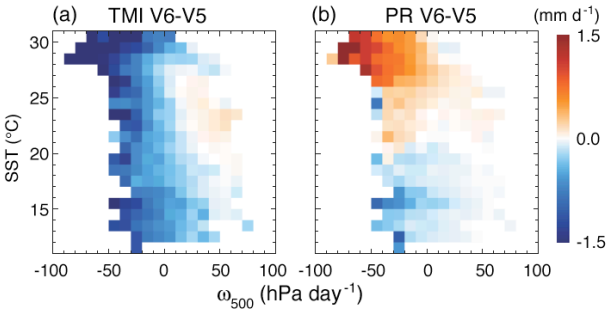

Fig. 3. *Differences between oceanic precipitation retrievals from the same product for different TRMM product versions. (a) TMI V6-V5 and (b) PR V6-V5. Comparisons use TMI and PR 3-month averages of monthly products 3B-31 and 3A-25 from 1998-2002 in a composite framework based on midtropospheric vertical velocity and SST.*

strong decrease in rain rate while those with lower SST and upward motion show a modest decrease in rain rate. In contrast, PR V6-V5 has a different pattern. PR rain rates increased for regions with higher SST and decreased for regions with SST <20°C. High SST and upward-motion regions, i.e., the regions with the highest precipitation rates, had the largest magnitude changes in rain rates between V5 and V6. To bring PR and TMI into better relative agreement, these changes were in opposite directions.

Figure 4a and b shows relative comparisons between TMI and PR for V5 and V6. Ideally these comparisons should show values near zero for all regions. In V5 there was a general tendency for TMI to overestimate precipitation compared to PR in upward-motion regions. In V6 the pattern is more complex (Fig. 4b). The relative importance of these differences to the global oceanic precipitation climatology is illustrated by weighting the difference pattern in Fig. 4b with the PDF of $_{500}$ and SST in Fig. 4c. The weighted difference pattern in Fig. 4d sums to 100% and indicates that the most important differences are for regions with SST >28°C and upward motion where TMI has lower rain rates than PR.

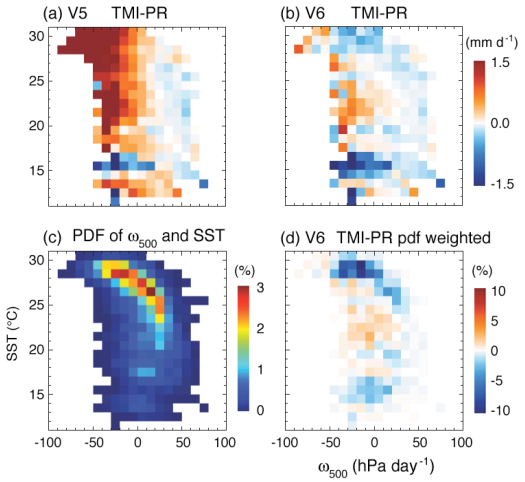

Fig. 4. *Relative differences between TMI-PR in V5 and V6 using composite framework as in Fig. 3. Average differences in rain rate are in mm day^{-1} for TMI-PR for (a) V5 and (b) V6. (c) Probability distribution of versus SST is scaled to sum to 100% and indicates more and less frequent combinations in the global climatology. (d) V6 rainfall differences weighed by pdf in (c). Entire plot (d) adds up to 100% of relative rainfall error between TMI and PR over oceans.*

6. REGIONAL PDF COMPARISONS

A closer look at the PDFs over ocean for specific geographic regions ~2.25 x 10^6 km^2 in scale over the 47-day period from 16 June to 1 August 2001 shows that the global ocean PDF is a superposition of the regional ocean PDFs. The degree of agreement between PR and TMI PDFs varies regionally. Some oceanic regional PDFs have degraded in plausibility between V5 and V6. Notably, several regional PDFs for TMI V6 ocean have a physically implausible bimodal structure

(a) Tropical Eastern Atlantic off Africa

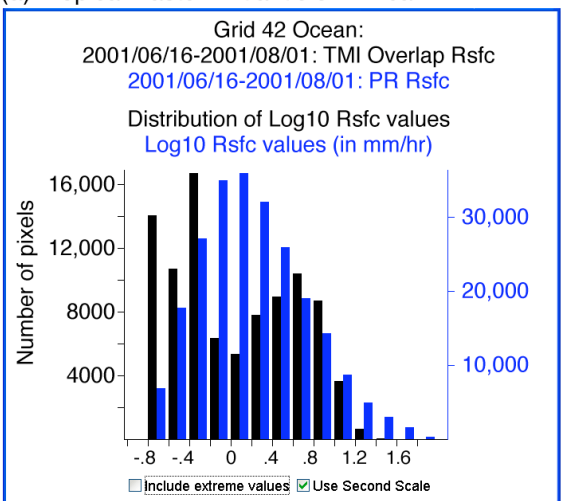

# Rainy Pixels:	105756.0	230796.0			
Min:	0.1	0.16	Max:	28.8	152.51
Mean:	2.28	3.74	Mean (log10):	-0.09	0.22
Std. Dev.:	3.27	7.28	Std. Dev (log10):	0.66	0.51
Skewness:	0.25	0.53	Kurtosis:	-1.22	-0.1

(b) SW Pacific between Australia and New Zealand

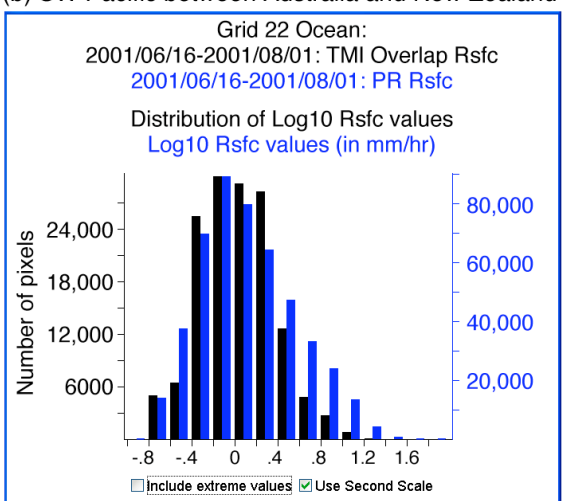

# Rainy Pixels:	139885.0	475304.0			
Min:	0.1	0.15	Max:	21.7	152.14
Mean:	1.53	2.41	Mean (log10):	0.03	0.13
Std. Dev.:	1.62	3.58	Std. Dev (log10):	0.37	0.45
Skewness:	-0.04	0.48	Kurtosis:	0.28	-0.26

Fig. 5. *Overlaid PDFs for TRMM V6 regional oceanic rain rates. PR rain rates are in blue and TMI swath overlapping PR are in black. PDFs represent accumulated statistics of instantaneous rain rates for 47 days of orbit products from 16 June – 1 August 2001 (pre-boost).*

(Fig. 5). The corresponding PR V5 and PR V6 PDFs are unimodal. The V6 TMI problematic PDFs appear in many regions with heavy tropical precipitation during June-August such as the tropical eastern Atlantic off the coast of Africa (Fig. 5a), the Bay of Bengal, and the east and west tropical Pacific. Some PDFs at higher latitudes also exhibit a bimodal character, such as the western Atlantic off the US coast. Other PDFs have the expected unimodal character such as the SW Pacific between the east coast of Australia and New Zealand (Fig. 5b).

7. CONCLUSIONS

Analysis of relative errors between TMI and PR V5 and V6 data sets reveals some steps forward and some steps backward in the TRMM algorithms. PDFs of rainrate are examined for the global ocean and land data sets and oceanic regional subsets. Additionally, changes in V5 versus V6 are examined in the framework of SST and midtropospheric vertical velocity.

TMI V6 over land represents a clear improvement over V5 (Fig. 1). The physically implausible discontinuous PDF in TMI V5 land has been remedied. V6 discrepancies between PR and TMI over land are at least partially related to differences in minimum detectable rain rates.

There is closer agreement between the global PDFs (Fig. 1) of TMI and PR rain rates over ocean in V6 as compared to V5. The direction and magnitude of the changes from V5 to V6 vary for different oceanic regions (Fig. 3). Both TMI and PR have changed most at high SST (>26°C) with TMI decreasing and PR increasing compared to their values in V5.

The relative differences between PR and TMI retrievals (Fig. 4) can be used to assess confidence in regional precipitation estimates. Four-year average 5° x 5° TMI-PR shows changing regional variations between V5 and V6 (Fig. 4) and overall better agreement between TMI and PR in V6.

Further examination shows that some regional PDFs of V6 TMI oceanic rain rate, such as for the tropical eastern Atlantic (Fig. 5), exhibit an implausible bimodal distribution of rain rates that is not present in either PR V6 or V5 products. These implausible bimodal characteristics in TMI oceanic rain rate PDFs are present in a subset of the oceanic tropical and midlatitude regions.

The seasonal cycle of rainfall from PR and TMI is a basic characteristic that is insensitive to absolute differences in rainfall amounts between PR and TMI. The magnitudes of the mean seasonal cycles decreased for TMI and increased for PR but the shape of the respective seasonal

cycles show little change between V5 and V6. PR and TMI seasonal cycles for the eastern Pacific ITCZ show seasonally dependent differences (Fig. 2). Seasonal precipitation magnitudes in July-September differ between TMI and PR from 0.3 to 0.8 mm day^{-1}. These relative differences in V6 are evidence of remaining problems in the physics of at least one of the satellite retrieval algorithms.

To be useful to the wider community, TRMM satellite precipitation retrievals must yield the right answers for the right reasons. Several types of relative error characteristics have improved between V5 and V6. However, changes to the TMI oceanic precipitation algorithm from V5 to V6 appear to have had unintended side effects that have degraded some regional TMI oceanic precipitation retrievals. The location and intensity of precipitation within these regions is such that these degradations are significant to global precipitation. The observed regional problems need further investigation, diagnosis, and correction.

Acknowledgments

The authors gratefully acknowledge Catherine Spooner, Dan Podhola, and Marc Michelsen for data processing and computer support for this paper. Candace Gudmundson edited the manuscript and Beth Tully refined the figures. The authors were supported by NASA grants NNG04GA65G and NNGO04GF33A.

References

Bony, S., J.-L. Dufresne, H. Le Treut, J.-J. Morcrette, and C. Senior, 2004: On dynamic and thermodynamic components of cloud changes. *Climate Dynamics*, **22**, 71-86.

Kummerow, C., W. Barnes, T. Kozu, J. Shue, and J. Simpson, 1998: The Tropical Rainfall Measuring Mission (TRMM) sensor package. *J. Atmos. Ocean. Tech.*, **15**, 809-817.

Smith, E. A., and coauthors, 1998: Results of the WetNet PIP-2 project. *J. Atmos. Sci.*, **55**, 1483-1536.

Tustison, B., D. Harris, and E. Foufoula-Georgiou, 2001: Scale issues in verification of precipitation forecasts. *J. Geophys. Res.*, **106**, 11,775-11,784.

Williams, K. D., M. A. Ringer, and C. A. Senior, 2003: Evaluating the cloud response to climate change and current climate variability. *Clim. Dyn.*, **20**, 705-721.